Uridine monophosphate synthetase enables eukaryotic *de novo* NAD$^+$ biosynthesis from quinolinic acid

Received for publication, May 8, 2017, and in revised form, May 25, 2017 Published, Papers in Press, May 30, 2017, DOI 10.1074/jbc.C117.795344

Melanie R. McReynolds, Wenqing Wang[1], Lauren M. Holleran, and Wendy Hanna-Rose[2]

From the Department of Biochemistry and Molecular Biology, The Pennsylvania State University, University Park, Pennsylvania 16802

Edited by Ruma Banerjee

NAD$^+$ biosynthesis is an attractive and promising therapeutic target for influencing health span and obesity-related phenotypes as well as tumor growth. Full and effective use of this target for therapeutic benefit requires a complete understanding of NAD$^+$ biosynthetic pathways. Here, we report a previously unrecognized role for a conserved phosphoribosyltransferase in NAD$^+$ biosynthesis. Because a required quinolinic acid phosphoribosyltransferase (QPRTase) is not encoded in its genome, *Caenorhabditis elegans* are reported to lack a *de novo* NAD$^+$ biosynthetic pathway. However, all the genes of the kynurenine pathway required for quinolinic acid (QA) production from tryptophan are present. Thus, we investigated the presence of *de novo* NAD$^+$ biosynthesis in this organism. By combining isotope-tracing and genetic experiments, we have demonstrated the presence of an intact *de novo* biosynthesis pathway for NAD$^+$ from tryptophan via QA, highlighting the functional conservation of this important biosynthetic activity. Supplementation with kynurenine pathway intermediates also boosted NAD$^+$ levels and partially reversed NAD$^+$-dependent phenotypes caused by mutation of *pnc-1*, which encodes a nicotinamidase required for NAD$^+$ salvage biosynthesis, demonstrating contribution of *de novo* synthesis to NAD$^+$ homeostasis. By investigating candidate phosphoribosyltransferase genes in the genome, we determined that the conserved uridine monophosphate phosphoribosyltransferase (UMPS), which acts in pyrimidine biosynthesis, is required for NAD$^+$ biosynthesis in place of the missing QPRTase. We suggest that similar underground metabolic activity of UMPS may function in other organisms. This mechanism for NAD$^+$ biosynthesis creates novel possibilities for manipulating NAD$^+$ biosynthetic pathways, which is key for the future of therapeutics.

NAD$^+$ is found in all living cells and is an essential coenzyme that impacts the entire metabolome (1). NAD$^+$ is involved in redox reactions where it carries electrons from one reaction to another and serves as a substrate for a group of enzymes called NAD$^+$ consumers that regulate a variety of key biological processes (2, 3). Thus, NAD$^+$ biosynthesis has proven to be an attractive and promising therapeutic target. However, exactly how NAD$^+$ homeostasis is maintained and the biological impact of manipulating NAD$^+$ biosynthetic pathways remain understudied. A complete understanding of the full complement of NAD$^+$ biosynthetic capacity as well as the consequences to the cell and the organism of manipulation of NAD$^+$ biosynthetic pathways is necessary to fully maximize the effectiveness of this target for therapeutic benefit.

A wide range of animals and yeast synthesize NAD$^+$ via *de novo* synthesis from the degradation of tryptophan via the kynurenine pathway (4). Tryptophan degradation typically occurs in the nervous system and liver of most mammals (5, 6). The derivatives of the kynurenine pathway have been commonly linked to both the progression and protection of neurological disorders and neurodegenerative diseases. Quinolinic acid (QA)[3] acts as an agonist to the *N*-methyl-D-aspartate (NMDA) glutamate receptors (7) and is characterized as a neurotoxin (8). In contrast, kynurenic acid (KYNA) acts as an antagonist to a spectrum of amino acid receptors and is considered to be a neuroprotective agent (7). The contrast between QA and KYNA and their roles in neurological disease states indicates the importance of maintaining kynurenine pathway homeostasis for healthy brain function (9). The relationship between NAD$^+$ *de novo* synthesis and the kynurenine pathway is important for normal metabolic function and homeostasis.

The genome of *Caenorhabditis elegans* encodes all the enzymes involved in the kynurenine pathway (Fig. 1*A*). However, the genome lacks the critical quinolinic acid phosphoribosyltransferase (QPRTase) ortholog that would convert QA into nicotinic acid mononucleotide (NaMN) for biosynthesis of NAD$^+$. Because the *C. elegans* lack an apparent QPRTase homolog, it has been assumed that this species lacks active NAD$^+$ *de novo* synthesis (2, 11, 12). We predict that organisms lacking a *de novo* NAD$^+$ synthesis pathway would be unable to clear the end product of tryptophan degradation, QA, a neurotoxin (7, 8). Thus, we examined the role of *de novo* synthesis in *C. elegans*. We discovered that the isotopic label supplied via Trp is incorporated into NAD$^+$. Blocking the kynurenine pathway lowers global NAD$^+$ levels compared with controls and prevents incorporation of the isotopic label, supplied via Trp, into NAD$^+$. We found that phenotypes that are dependent on NAD$^+$ levels could be reversed upon supplementation with QA

This work was supported by National Institutes of Health Grant GM086786 (to W. H. R.). The authors declare that they have no conflicts of interest with the contents of this article. The content is solely the responsibility of the authors and does not necessarily represent the official views of the National Institutes of Health.

[1] Present address: ABLife Inc., Wuhan, Hubei 430075, China.

[2] To whom correspondence should be addressed: 104D Life Science Bldg., University Park, PA 16802. Tel.: 814-865-7904; E-mail: wxh21@psu.edu.

[3] The abbreviations used are: QA, quinolinic acid; 3HAA, 3-hydroxyanthranilate; Kyn, kynurenine; KYNU-1, kynureninase; NA, nicotinic acid; QPRTase, quinolinic acid phosphoribosyltransferase; UMPS-1, uridine monophosphate synthetase; F, forward; R, reverse.

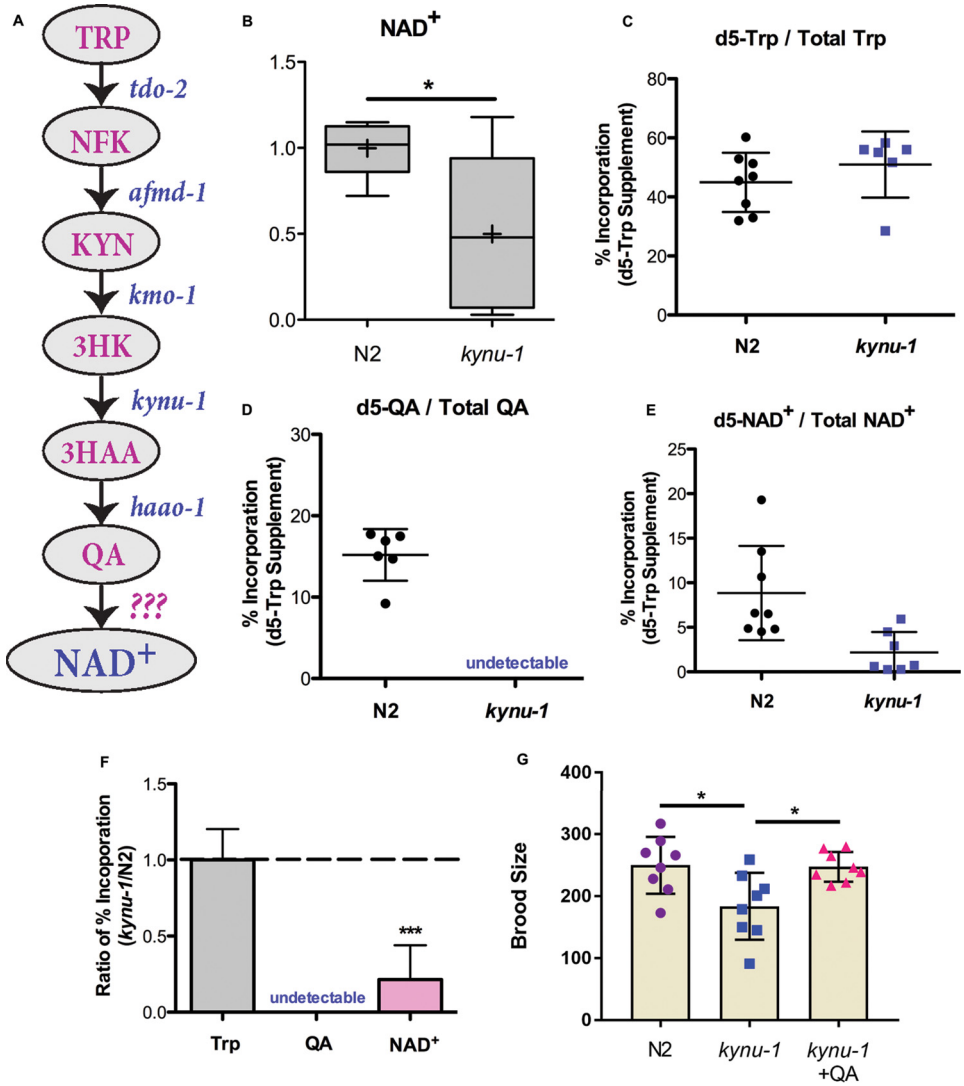

Figure 1. NAD$^+$ *de novo* synthesis contributes to NAD$^+$ biocapacity and reproduction. *A,* schematic of NAD$^+$ *de novo* synthesis in *C. elegans*. *NFK* is *N*-formylkynurenine; *3HK* is hydroxy-L-kynurenine. *B,* LC-MS measurements of relative levels of NAD$^+$ in N2 and *kynu-1*(*tm4924*) mutant animals. *Boxes* show the upper and lower quartile values; + indicates the mean value, and *line* indicates the median. *Error bars* indicate the maximum and minimum of the population distribution. *, $0.01 < p < 0.05$; calculated with Welch's two sample *t* test. *C–E,* percent incorporation of isotope label from d_5-Trp supplementation into the Trp pool (*C*), the QA pool (*D*), and NAD$^+$ pool (*E*) in N2 and *kynu-1*(*tm4924*) mutant animals. *Dots* represent each biological replicate of N2 and *kynu-1*(*tm4924*) mutant animals sampled after 4 h of exposure to d_5-Trp. + indicates the mean value, and *error bars* are S.D. The peak area for total QA was undetectable in *kynu-1* mutants, likely as a result of blocking the biosynthesis pathway. *F,* ratio of percent isotope label incorporated into Trp, QA, and NAD$^+$ in *kynu-1*(*tm4924*) mutants compared with N2. *Error bars* indicate S.D. ***, $p < 0.001$; calculated with Welch's two sample *t* test. *G,* progeny production is reported for N2 control and *kynu-1*(*tm4924*) mutant animals and *kynu-1* mutant animals supplemented with 20 mM QA. *Error bars* indicate S.D. *, $0.01 < p < 0.05$, calculated with Student's *t* test.

and other kynurenine metabolites. Furthermore, we identified a candidate enzyme that is required for incorporation of isotopic label supplied via QA into NAD$^+$. Finally, we connected *de novo* NAD$^+$ synthesis to fecundity. This evidence supports the hypothesis that NAD$^+$ *de novo* synthesis is active and contributes to NAD$^+$ biosynthetic capacity and homeostasis of *C. elegans*.

Results

NAD$^+$ de novo synthesis contributes to biosynthetic capacity and reproduction

To investigate whether the kynurenine pathway contributes to NAD$^+$ *de novo* biosynthesis in *C. elegans*, we examined the effect of loss of the pathway on global NAD$^+$ levels. *kynu-1* encodes kynureninase and is required for conversion of 3-hydroxy-L-kynurenine to 3-hydroxyanthranilic acid (3HAA) and indirectly for formation of QA (13). The *kynu-1*(*tm4924*) mutants, which have a deletion of three internal exons of the *kynu-1* gene (14), have decreased global NAD$^+$ levels compared with controls (Fig. 1*B*). We conclude that the kynurenine pathway contributes to NAD$^+$ homeostasis in *C. elegans* perhaps by contributing to biosynthetic capacity.

To directly test whether *de novo* NAD$^+$ synthesis from tryptophan via QA occurs, we used isotopically labeled metabolic tracers. After short-term supplementation of cultures with deuterium-labeled Trp, we successfully detected isotope label in the tryptophan pool (Fig. 1*C*). Furthermore, we detected isotope label in 15% of the QA pool and in an average of 9% of the

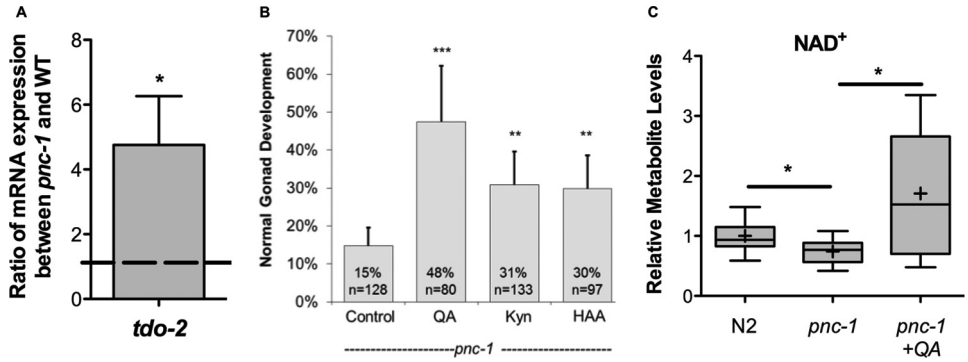

Figure 2. Supplementation with NAD$^+$ *de novo* precursors reverses NAD$^+$-dependent phenotypes. *A,* ratio of *tdo-2* mRNA levels in *pnc-1*(*pk9605*) mutants and N2 controls. *tdo-2* encodes the enzyme that catalyzes the rate-limiting step in the kynurenine pathway. *, $0.01 < p < 0.05$, calculated with Student's *t* test. *B,* supplementation of 20 mM QA, Kyn, and 3HAA to *pnc-1*(*pk9605*) mutants restores the gonad developmental delay. For histograms, *error bars* are S.D. **, $0.001 < p < 0.01$; ***, $p < 0.001$; calculated with Fisher's exact test. *C,* supplementation of 20 mM QA to *pnc-1*(*pk9605*) mutants restores NAD$^+$ levels. LC-MS measurements of relative levels of NAD$^+$ and in N2 and *pnc-1*(*pk9605*) mutant. Plots are described in legend to Fig. 1*B*. *, $0.01 < p < 0.05$; calculated with Welch's two sample *t* test.

NAD$^+$ pool (Fig. 1, *D* and *E*). This demonstrates the flow of label from Trp to NAD$^+$ via a *de novo* synthesis pathway. Next, we investigated whether this flow was dependent on an active kynurenine pathway. We predicted that loss of *kynu-1* would block incorporation of Trp-supplied label into NAD$^+$. The Trp pool was isotopically labeled in *kynu-1* mutants at a level similar to the control (Fig. 1*C*). As expected, mutation of *kynu-1* decreased the efficiency of label incorporation into NAD$^+$ more than 2-fold relative to controls (Fig. 1, *E* and *F*). Labeled QA was below the detection limit upon removal of *kynu-1* activity (Fig. 1*D*). This supports our hypothesis that NAD$^+$ *de novo* synthesis from tryptophan is actively contributing to NAD$^+$ biosynthetic capacity in *C. elegans*, although the organism lacks a functional QPRTase homolog in genome.

We next asked whether NAD$^+$ *de novo* synthesis from tryptophan was functionally important by examining fecundity. We observed a decrease in progeny production in *kynu-1* mutants compared with controls (Fig. 1*G*). However, supplementation with QA, the kynurenine pathway end product and the NAD$^+$ *de novo* synthesis precursor, restored the brood size in *kynu-1* mutants, supporting a functional role for *de novo* NAD$^+$ biosynthesis in fecundity (Fig. 1*G*).

Supplementation with de novo precursors reverses NAD$^+$-dependent phenotypes

We previously reported that reduced levels of NAD$^+$ caused by the lack of salvage synthesis in *pnc-1* mutants impair reproductive development in *C. elegans* (15). Although the levels of nicotinic acid (NA), the product of PNC-1, are reduced almost 20-fold in the mutant, NAD$^+$ levels are only reduced by about 30% (15). Therefore, we hypothesized that alternative NAD$^+$ biosynthetic pathways could respond to the loss of salvage synthesis to maintain global NAD$^+$ levels. To investigate this hypothesis, we examined expression of *tdo-2,* which encodes the enzyme that catalyzes the rate-limiting step of the kynurenine pathway. We detected a greater than 4-fold increase in *tdo-2* transcript levels in *pnc-1* mutants (Fig. 2*A*), supporting an active and functional role for the *de novo* pathway in NAD$^+$ homeostasis in *C. elegans*. We further reasoned that an increase in available *de novo* precursors in combination with the detected up-regulation of *tdo-2* might ameliorate *pnc-1* phenotypes. To test this hypothesis, we supplemented *pnc-1* mutant animals with QA, Kyn, and 3HAA. All three supplements improved the reproductive gonad delay phenotype of *pnc-1* mutants (Fig. 2*B*). Supplementation with QA also boosted the global levels of NAD$^+$ in *pnc-1* mutants (Fig. 2*C*). We conclude that boosting *de novo* synthesis can reverse NAD$^+$-dependent phenotypes in *pnc-1* mutants and that *de novo* synthesis functionally contributes to NAD$^+$ homeostasis.

UMPS-1 contributes to NAD$^+$ biosynthesis

If *de novo* synthesis is indeed active in *C. elegans,* then how is QA used as a substrate without the QPRTase enzyme? We hypothesized that another phosphoribosyltransferase encoded in the genome would be required to synthesize NAD$^+$ from QA. The *C. elegans* genome contains seven annotated phosphoribosyltransferases. Interestingly, only UMPS-1 (uridine monophosphate synthetase) has a domain structure similar to QPRTase, with both the phosphoribosyltransferase domain and a carboxylase domain. We specifically asked whether *umps-1* is functionally involved in NAD$^+$ biosynthesis by determining whether it is required for QA supplementation to rescue *pnc-1* phenotypes or for incorporation of isotope label supplied via Trp into NAD$^+$. As noted above, QA supplementation rescues gonad developmental delay in *pnc-1* mutants. We predicted that if *umps-1* played a role in *de novo* NAD$^+$ synthesis, then loss of *umps-1* would block the ability of QA but not NA to restore normal gonad development to a proportion of *pnc-1* mutants. To test this prediction, we used the deletion allele *ok2703*, which removes a portion of the 3rd as well as the entire final (4th) exon of the *umps-1* gene. As expected, whereas NA increases the proportion of normal gonad development for both *pnc-1* mutants and *umps-1*(*ok2703*);*pnc-1* double mutants, QA affects only the *pnc-1* mutant but not the *umps-1*(*ok2703*);*pnc-1* double mutant (Fig. 3*A*). Next, we predicted that loss of *umps-1* would lower NAD$^+$ steady-state levels and increase QA steady-state levels if it were participating in *de novo* NAD$^+$ biosynthesis at the step typically catalyzed by QPRTase. Indeed, global NAD$^+$ levels are decreased and QA steady-state levels are increased in *umps-1*(*ok2703*) mutants compared with controls (Fig. 3, *B* and *C*). The decrease in NAD$^+$ levels is similar to that observed in *kynu-1* mutants (Fig. 1*B*).

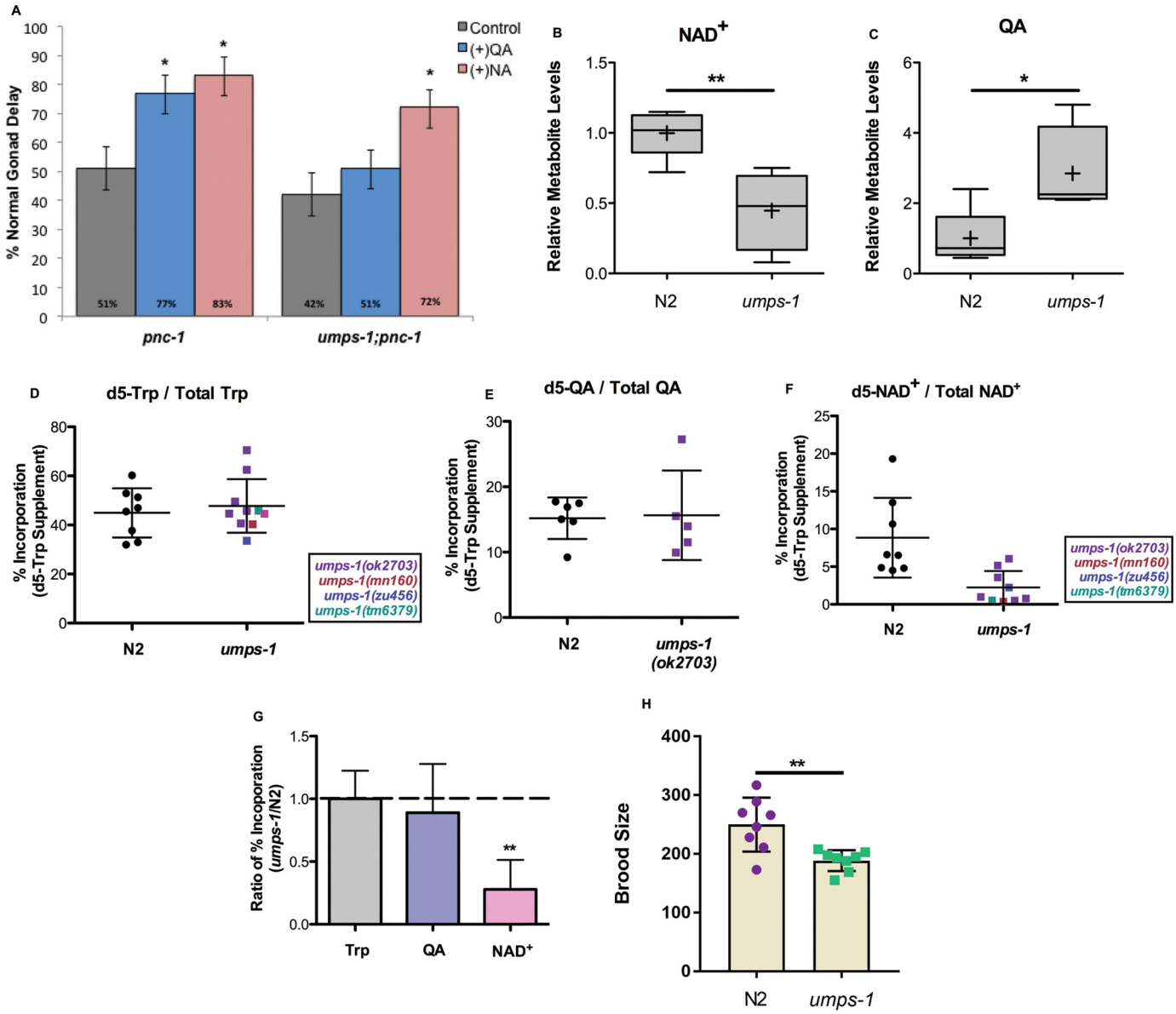

Figure 3. UMPS-1 is required for NAD$^+$ *de novo* synthesis. *A,* supplementation of QA to *pnc-1*(*pk9605*) mutants restores the gonad developmental delay but has no effect on *umps-1*(*ok2703*);*pnc-1*(*pk9605*) animals, whereas supplementation of NA restores gonad development in both genetic backgrounds. Note that the penetrance of the gonad development phenotype is influenced by food type (15, 18). The penetrance is lower (more normal animals) in this experiment than that reported in Fig. 2*B*. These animals were supplemented on culture plates with UV-killed food, whereas the supplementation reported in Fig. 2*B* was performed in liquid culture with heat-killed food, which exacerbates the phenotype. *Error bars* are S.D. *, $0.01 < p < 0.05$; **, $0.001 < p < 0.01$; ***, $p < 0.001$; calculated with Fisher's exact test. *B* and *C,* LC-MS measurements of relative levels of NAD$^+$ (*B*) and QA (*C*) in N2 and *umps-1*(*ok2703*) mutant animals. Plots are described in legend to Fig. 1*B*. *, $0.01 < p < 0.05$; **, $0.001 < p < 0.01$; calculated with Welch's two sample *t* test. *D–F,* percent incorporation of isotope label from d_5-Trp supplementation into the Trp pool (*D*), the QA pool (*E*), and NAD$^+$ pool (*F*) in N2 and *umps-1* mutant animals. Data derived from a variety of alleles of *umps-1* are provided and differentiated via the color code on the figure panel. *G,* ratio of percent isotope label incorporated into Trp, QA, and NAD$^+$ in *umps-1*(*ok2703*) mutants compared with N2. *Error bars* indicate S.D. Plots are as described in Fig. 1*B*. **, $0.001 < p < 0.01$, calculated with Welch's two sample *t* test. *H,* progeny production is reported for N2 control and *umps-1*(*ok2703*) mutant animals. **, $0.001 < p < 0.01$; calculated with Student's *t* test.

If UMPS-1 substitutes for the missing QPRTase, we predict that loss of *umps-1* would block incorporation of isotope label provided via Trp into NAD$^+$. We exposed control animals and *umps-1*(*ok2703*) mutants to deuterium-labeled tryptophan for 4 h (Fig. 3*D*), and we measured incorporation of deuterium label into the pool of Trp, QA, and NAD$^+$. In contrast to loss of *kynu-1*, *umps-1* does not block label incorporation into QA (Fig. 3*E*), as expected for a gene acting downstream of QA in the pathway. However, *umps-1*(*ok2703*) decreased the proportion of the NAD$^+$ pool that became labeled (Fig. 3*F*). To ensure that the observed effects associated with the *ok2703* deletion were specifically attributable to the deletion within the *umps-1* gene, we also examined three additional *umps-1* alleles, *zu456*, *tm6379*, and *mn160*, for their effect on isotope label incorporation into NAD$^+$ and found consistent results (Fig. 3, *F* and *G*). This metabolic tracing analysis provides key evidence that *de novo* NAD$^+$ synthesis from tryptophan contributes to NAD$^+$ biosynthesis and that UMPS-1 is required for *de novo* synthesis. In support of this observation, loss of *umps-1*(*ok2703*) disrupts fecundity (Fig. 3*H*). This further suggests that UMPS-1 can substitute as the QPRTase missing from the *C. elegans* genome. These data highlight functional conservation of *de novo* NAD$^+$

biosynthesis and demonstrate an unexpected flexibility for application of a pyrimidine biosynthesis enzyme in contributing to NAD$^+$ biosynthesis.

Discussion

NAD$^+$ homeostasis is critical for healthy metabolic function and important biological stress responses. Not surprisingly, cells use more than one biosynthetic route for the production of NAD$^+$ (1). All of the pathways that contribute to NAD$^+$ biosynthetic capacity are also highly conserved throughout evolution, alluding to the importance of NAD$^+$ as a cellular hub for metabolism in all organisms (1–3). Our results highlight the conservation of the NAD$^+$ biosynthetic pathways and expand our knowledge of comprehensive mechanisms for NAD$^+$ biosynthesis.

Despite the absence of what was assumed to be a key enzyme in their genome, *C. elegans* maintain an intact pathway for NAD$^+$ *de novo* synthesis. We used stable isotope metabolic tracer analysis to directly demonstrate metabolite flow from Trp to NAD$^+$ via QA, and we demonstrated the contribution of the pathway to maintenance of global NAD$^+$ levels as well as function in fecundity. Using stable isotope metabolic tracers combined with genetic analysis, we also demonstrated that *umps-1* is required for this *de novo* synthesis of NAD$^+$, suggesting that the well-conserved enzyme uridine monophosphate synthase, known for its primary role in pyrimidine biosynthesis, likely plays a dual role in *C. elegans*. This second role in NAD$^+$ biosynthesis highlights the possibility for the contribution of similar underground metabolic activity (16) to NAD$^+$ biosynthetic capacity in other organisms, even humans.

One of the reasons we predicted that *C. elegans* may have an active *de novo* NAD$^+$ synthesis pathway is that a method to clear the end product of the kynurenine pathway, QA, a known neurotoxin, would be necessary. It is interesting to note that *Drosophila* also lack a QPRTase ortholog. However, the enzyme 3-hydroxyanthranilic acid dioxygenase, required for production of QA, is also missing from the *Drosophila* genome, suggesting that *Drosophila* do not produce QA and thus may actually lack this otherwise conserved *de novo* pathway for NAD$^+$ biosynthesis. Alternatively, given the importance of *de novo* synthesis to most metazoans, it would not be surprising to find intact mechanisms for *de novo* synthesis of NAD$^+$ in *Drosophila*.

We have concluded that *umps-1* is required for *de novo* NAD$^+$ biosynthesis. However, we also considered the possibility that perturbations to pyrimidine biosynthesis indirectly negatively affect NAD$^+$ biosynthesis. Although we have not formally ruled this out, we favor a direct model because we have demonstrated that UMPS-1 specifically acts between QA and NAD$^+$ in biosynthesis, but yet is not downstream of nicotinic acid in ameliorating the NAD-dependent gonad delay phenotype of the NAD$^+$ salvage biosynthesis mutant *pnc-1*.

We previously reported that salvage NAD$^+$ synthesis is critical for the normal progression of gonad development, for full fecundity, and for efficient glucose metabolism in the cytosol (12, 15, 17, 18). Interestingly, loss of NAD$^+$ *de novo* synthesis also resulted in decreased progeny production compared with wild type. Supplementation with NAD$^+$ precursors was able to reverse the brood size defect in *kynu-1* mutants, supporting the importance of NAD$^+$ biosynthesis for normal reproduction. Both *de novo* NAD$^+$ synthesis and salvage NAD$^+$ synthesis (17) are involved in fecundity. This highlights the role of maintaining global NAD$^+$ biosynthetic capacity for reproduction.

Our results also highlight the relevance of potential homeostatic mechanisms in response to targeting NAD$^+$ biosynthetic pathways for therapeutic use. For instance, inhibiting salvage NAD$^+$ synthesis can result in increased *de novo* synthesis. Similarly, targeting the kynurenine pathway in neurological disorders could result in altered NAD$^+$ synthesis. Homeostatic interactions among NAD$^+$ biosynthetic pathways should be taken into consideration when manipulating NAD$^+$ biosynthesis and metabolism for therapeutic benefits.

Experimental procedures

C. elegans culture and strains

C. elegans strains were maintained under standard conditions at 20 °C (19) with *Escherichia coli* OP50 or UV-irradiated OP50 serving as the food source. N2 is the reference control strain. UV-irradiated OP50 plates were prepared using a 999-s exposure in a GS Gene Linker UV Chamber (Bio-Rad) (12, 18). Complete killing of the *E. coli* was confirmed by absence of growth on LB agar after overnight incubation at 37 °C. The following strains and alleles were used: *pnc-1*(*pk9605*) (12), *kynu-1*(*tm4924*), and *umps-1*(*ok2703, mn160, tm6379,* and *zu456*). *ok2703* also deletes a portion of the N terminus of the neighboring gene, *spp-1*, which encodes an antibacterial caenopore (21). Strains were obtained from the CGC and Mitani Lab/National BioResource Project, Japan.

Metabolite supplementation

NA (Alfa Aesar, Tewksbury, MA) and QA (MP Biomedicals, Santa Ana, CA) supplementations were performed on culture plates. We added filter-sterilized 25 mM stock solution of NA and QA to UV-irradiated plates and incubated plates at room temperature for 2–3 days to allow chemicals to diffuse before use.

QA, Kyn (Sigma), and HAA (Sigma) supplementations were performed in small-volume liquid culture because of limited availability of supplements. We first plated synchronized L1 animals on UV-irradiated OP50 plates for 24 h. 2–3 plates of synchronized L3 animals were then collected with M9 solution and pelleted. To the pellet we added 5 μl of concentrated heat-killed OP50 culture, supplement stock solution diluted to the experimental concentration, and M9 to a final volume of 100 μl. Stock solutions were as follows: 20 mM QA, 20 mM Kyn, or 20 mM 3HAA. Liquid culture solutions were incubated at room temperature for 48 h with gentle rocking. Finally animals were plated on UV-irradiated OP50 plates, and gonad development was scored when animals reached mid-L4 stage.

Phenotypic analysis, gonad developmental delay

Gonad developmental delay phenotype was scored as reported previously (12). Briefly, mid-L4 stage animals with an open lumen in both the vulva and the uterus were reported as normal. "Delayed" animals are those that do not yet have an

open uterine lumen when the vulva lumen achieves its characteristic mid-L4 stage morphology. We plated synchronized L1 animals on NGM plates of targeted condition, scored the gonad delay when they reached mid-L4 stage, and calculated the percentage of normal animals.

Brood size

Young L3 stage animals were individually plated, and production of progeny was counted for 4 days after reaching adulthood.

Targeted metabolomics

We performed targeted LC-MS metabolomics analysis at the Metabolomics Core Facility at Pennsylvania State University. ~50 μl of worms were collected in double distilled H_2O, flash-frozen in liquid nitrogen, and stored at −80 °C. 15-μl samples were extracted in 1 ml of 3:3:2 acetonitrile/isopropyl alcohol/H_2O with 1 μM chlorpropamide as internal standard. Samples were homogenized using a Precellys^{TM} 24 homogenizer. Extracts from samples were dried under vacuum, resuspended in HPLC Optima Water (Thermo Fisher Scientific, Waltham, MA), and divided into two fractions, one for LC-MS and one for BCA protein analysis. Samples were analyzed by LC-MS using a modified version of an ion pairing reversed phase negative ion electrospray ionization method (10). Samples were separated on a Supelco (Bellefonte, PA) Titan C18 column (100 × 2.1 mm, 1.9-μm particle size) using a water/methanol gradient with tributylamine added to the aqueous mobile phase. The LC-MS platform consisted of a Dionex Ultimate 3000 quaternary HPLC pump, a Dionex 3000 column compartment, a Dionex 3000 autosampler, and an Exactive plus orbitrap mass spectrometer controlled by Xcalibur 2.2 software (all from Thermo Fisher Scientific, San Jose, CA). The HPLC column was maintained at 30 °C at flow rate of 200 μl/min. Solvent A was 3% aqueous methanol with 10 mM tributylamine and 15 mM acetic acid; solvent B was methanol. The gradient was 0 min, 0% B; 5 min, 20% B; 7.5 min, 20% B; 13 min, 55% B; 15.5 min, 95% B; 18.5 min, 95% B; 19 min, 0% B; and 25 min, 0% B. The orbitrap was operated in negative ion mode at maximum resolution (140,000) and scanned from m/z 85 to m/z 1000. Metabolite levels were corrected to protein concentrations determined by BCA assay (Thermo Fisher Scientific).

Metabolic tracing with stable isotopes

Stable isotope d_5-tryptophan (Santa Cruz Biochemicals, Dallas, TX) was used as the metabolic tracer. To collect isotopic Trp-treated *C. elegans*, mixed-stage worms were plated on UV-irradiated OP50 plates and incubate at 20 °C for 72 h. Worms were then collected with M9 solution and pelleted. To the pellet we added 1 ml of concentrated heat-killed OP50 culture, 100 μl of 100 mM isotopic Trp, and M9 to a final volume of 2 ml. Liquid culture solutions were incubated at room temperature for 4 h with gentle rocking. Worms and heat-killed OP50 were separately collected by centrifuging and washed with 15 ml of autoclaved water three times. Approximately 30–40 μl of worm pellets were obtained for each sample. Targeted LC-MS metabolomics analysis was performed to measure isotope incorporation.

Quantitative real-time PCR

RNA was extracted from N2 control and *pnc-1* mutant animals cultured on OP50 plates using TRIzol Reagent (Life Technologies, Inc.). 2 μg of total RNA, quantified by NanoDrop NA-1000 spectrophotometer (NanoDrop Technologies, Wilmington, DE), was used for reverse transcription with the High Capacity cDNA Reverse Transcription kit (Applied Biosystems, Foster City, CA). Three genes, *cdc-42*, *pmp-3*, and *tba-1*, were used as internal reference control (20). Real-time quantitative PCR amplifications for test and reference genes were carried out using 7.5 μl of SYBR Green (PerfeCTa SYBR Green Super Mix with ROX, Quanta Biosciences Beverly, MA), 0.6 μl of forward and reverse primers, 1.3 μl of distilled H_2O, and 5 μl of diluted cDNA for each sample in a total of 15 μl. Amplification was carried out in a 7300 real-time PCR system (Applied Biosystems, Foster City, CA) with initial polymerase activation at 95 °C for 10 min, followed by 40 cycles of 95 °C for 15 s denaturation, 60 °C for 60 s for primer-specific annealing, and elongation. After 40 cycles, melting curve analysis was carried out (60–95 °C) to verify the specificity of amplicons. The following primers were used: for internal reference genes, *cdc-42*-F (5′-ctgctggacaggaagattacg-3′) and *cdc-42*-R (5′-ctcggacattctcgaatgaag-3′); *pmp-3*-F (5′-gttcccgtgttcatcactcat-3′) and *pmp-3*-R (5′-acaccgtcgagaagctgtaga-3′); *tba-1*-F (5′-gtacactccactgatctctgctgacaag-3′) and *tba-1*-R (5′-ctctgtacaagaggcaaacagccatg-3′), and for test genes, *tdo-2*-F (5-tgtccgtatttgggttctgg-3′) and *tdo-2*-R (5′-accaactaacctgtagatattcggaa-3′).

Statistical analysis

Fisher's exact test was carried out to determine p values for the gonad developmental delay phenotype. For quantification of the fecundity defect and gene expression, p values were calculated using Student's t test. Welch's two-sample t test to calculate p values was used for LC-MS analysis. In all figures the following were used: §, $0.05 < p < 0.1$; *, $0.01 < p < 0.05$; **, $0.001 < p < 0.01$; ***, $p < 0.001$.

Author contributions—M. R. M., W. W., and W. H. R. conceived and planned the experiments. M. R. M., W. W., and L. H. performed the experiments and analyzed the data. M. R. M. and W. H. R. wrote the manuscript.

Acknowledgments—We thank A. Patterson and P. Smith and the Pennsylvania State Metabolomics Core Facility, Huck Institutes of the Life Sciences, for technical assistance and advice. tm alleles were provided by the Mitani Lab through the National Bio-Resource Project of the Ministry of Education, Culture, Sports, Science and Technology, Japan. Other strains were provided by the Caenorhabditis Genetics Center, which is funded by National Institutes of Health Office of Research Infrastructure Programs Grant P40 OD010440.

References

1. de Figueiredo, L. F., Gossmann, T. I., Ziegler, M., and Schuster, S. (2011) Pathway analysis of NAD$^+$ metabolism. *Biochem. J.* **439,** 341–348
2. Gossmann, T. I., Ziegler, M., Puntervoll, P., de Figueiredo, L. F., Schuster, S., and Heiland, I. (2012) NAD$^+$ biosynthesis and salvage–a phylogenetic perspective. *FEBS J.* **279,** 3355–3363
3. Sauve, A. A. (2008) NAD$^+$ and vitamin B3: from metabolism to therapies. *J. Pharmacol. Exp. Ther.* **324,** 883–893

4. Ball, H. J., Yuasa, H. J., Austin, C. J., Weiser, S., and Hunt, N. H. (2009) Indoleamine 2,3-dioxygenase-2; a new enzyme in the kynurenine pathway. *Int. J. Biochem. Cell Biol.* **41,** 467–471
5. Magni, G., Amici, A., Emanuelli, M., Orsomando, G., Raffaelli, N., and Ruggieri, S. (2004) Enzymology of NAD$^+$ homeostasis in man. *Cell. Mol. Life Sci.* **61,** 19–34
6. Bogan, K. L., and Brenner, C. (2008) Nicotinic acid, nicotinamide, and nicotinamide riboside: a molecular evaluation of NAD$^+$ precursor vitamins in human nutrition. *Annu. Rev. Nutr.* **28,** 115–130
7. Sas, K., Robotka, H., Toldi, J., and Vécsei, L. (2007) Mitochondria, metabolic disturbances, oxidative stress and the kynurenine system, with focus on neurodegenerative disorders. *J. Neurol. Sci.* **257,** 221–239
8. Stone, T. W., and Perkins, M. N. (1981) Quinolinic acid: a potent endogenous excitant at amino acid receptors in CNS. *Eur. J. Pharmacol.* **72,** 411–412
9. Schwarcz, R., and Pellicciari, R. (2002) Manipulation of brain kynurenines: glial targets, neuronal effects, and clinical opportunities. *J. Pharmacol. Exp. Ther.* **303,** 1–10
10. Lu, W., Clasquin, M. F., Melamud, E., Amador-Noguez, D., Caudy, A. A., and Rabinowitz, J. D. (2010) Metabolomic analysis via reversed-phase ion-pairing liquid chromatography coupled to a stand alone orbitrap mass spectrometer. *Anal. Chem.* **82,** 3212–3221
11. Rongvaux, A., Andris, F., Van Gool, F., and Leo, O. (2003) Reconstructing eukaryotic NAD metabolism. *BioEssays* **25,** 683–690
12. Vrablik, T. L., Huang, L., Lange, S. E., and Hanna-Rose, W. (2009) Nicotinamidase modulation of NAD$^+$ biosynthesis and nicotinamide levels separately affect reproductive development and cell survival in *C. elegans*. *Development* **136,** 3637–3646
13. Majewski, M., Kozlowska, A., Thoene, M., Lepiarczyk, E., and Grzegorzewski, W. J. (2016) Overview of the role of vitamins and minerals on the kynurenine pathway in health and disease. *J. Physiol. Pharmacol.* **67,** 3–19
14. *C. elegans* Deletion Mutant Consortium (2012) Large-scale screening for targeted knockouts in the *Caenorhabditis elegans* genome. *G3* **2,** 1415–1425
15. Wang, W., McReynolds, M. R., Goncalves, J. F., Shu, M., Dhondt, I., Braeckman, B. P., Lange, S. E., Kho, K., Detwiler, A. C., Pacella, M. J., and Hanna-Rose, W. (2015) Comparative metabolomic profiling reveals that dysregulated glycolysis stemming from lack of salvage NAD$^+$ biosynthesis impairs reproductive development in *Caenorhabditis elegans*. *J. Biol. Chem.* **290,** 26163–26179
16. D'Ari, R., and Casadesús, J. (1998) Underground metabolism. *BioEssays* **20,** 181–186
17. Huang, L., and Hanna-Rose, W. (2006) EGF signaling overcomes a uterine cell death associated with temporal mis-coordination of organogenesis within the *C. elegans* egg-laying apparatus. *Dev. Biol.* **300,** 599–611
18. Vrablik, T. L., Wang, W., Upadhyay, A., and Hanna-Rose, W. (2011) Muscle type-specific responses to NAD$^+$ salvage biosynthesis promote muscle function in *Caenorhabditis elegans*. *Dev. Biol.* **349,** 387–394
19. Brenner, S. (1974) The genetics of *Caenorhabditis elegans*. *Genetics* **77,** 71–94
20. Hoogewijs, D., Houthoofd, K., Matthijssens, F., Vandesompele, J., and Vanfleteren, J. R. (2008) Selection and validation of a set of reliable reference genes for quantitative sod gene expression analysis in *C. elegans*. *BMC Mol. Biol.* **9,** 9
21. Bányai, L., and Patthy, L. (1998) Amoebapore homologs of *Caenorhabditis elegans*. *Biochim. Biophys. Acta* **1429,** 259–264